

₁ _typical_2012 _neutron_2010 _neutron_1999 _comparative_1982 _geant4simulation_2003 _collaboration_-
₂ geant4_2011 _geant4_2006 _physics_2012 _reference_2008 _detector_2012 _scintillations_1951 _recoil_1980

3

Energy Deposition in Polymers

4

Matthew J. Urffer

5

December 10, 2012

6

Todo list

7

Expand this section 10

8	Contents	
9	1 Introduction	7
10	2 Previous Work	8
11	2.1 Spectra Measurements	8
12	2.2 Single Collision Energy Loss	8
13	3 Introduction to GEANT4	10
14	3.1 Organization of the GEANT4 Toolkit	10
15	3.2 GEANT4 Tracking and Secondaries	10
16	4 Methods	12
17	4.1 GEANT4 Implementation	12
18	4.1.1 Detector Geometry	12
19	4.1.2 Physics Lists	13
20	4.1.3 Primary Event Generator	14
21	4.2 Sensitive Detectors and Hits	15
22	4.3 Analysis	17
23	4.4 Determination of Energy Deposition	18
24	5 Simulation Validation	21
25	5.1 Energy Deposition Validation	21
26	5.2 Spectra Validation	21
27	6 Results	23
28	6.1 Energy Deposition	23
29	6.2 Secondary Electron Energy Distribuion	23
30	7 Conclusions	24

31 List of Figures

32	1	Spectra properties as a function of film thickness	8
33	2	Gamma intrinsic efficiency (dashed lines) plotted against neutron counts (solid)	8
34	3	Single-collision energy loss spectra for electrons in water [?]	8
35	4	Average and median energy transfer in liquid water as functions of incident-electron energy [?]	9
36	5	World, Calorimeter, Layer and Absorber and Gap	13
37	6	10 Layer Detector with a simulated gamma event	13
38	7	Single Collision Energy Loss of Water	21
39	8	Gamma Simulation Agreement	22
40	9	Neutron Simulation Agreement	22
41	10	Simulated Energy Depositon for a Single Film (gammas)	23
42	11	Simulated Energy Depositon for a Single Film (neutrons)	23
43	12	Simulated kinetic energies of electrons from ^{60}Co interactions	23
44	13	Comparison between average neturon and gamma energy deposition	24

45 List of Tables

46	1	Replacement Detector Requirements [?]	7
47	2	Maximum Energy of Secondary Electrons from Compton Scattering	7

48 Listings

49	1	Tracking Example	11
50	2	World Physical Volume	12
51	3	Calorimeter Volume	12
52	4	Layer Volume	13
53	5	Absorber and Gap Volumes	13
54	6	Implemented Physics List	14
55	7	Implemented Physics List	14
56	8	Primary Event Generator	14
57	9	Generate Primaries	15
58	10	Calorimeter Hit	15
59	11	Sensitive Detector	16
60	12	Creating Sensitive Detectors	17
61	13	Event Action	17
62	14	Run Action	18
63	15	Process Hit Collection	18
64	16	Run Macro	19

1 Introduction

A typical day in 2011 saw 932,456 people enter into the U.S. (258,191 by air 48,073 by sea, and 621,874 by land) in addition to 64,483 truck, rail and sea containers and 253,821 privately-owned vehicles [?]. Any one of these could be a pathway of special nuclear material to enter the U.S. The interdiction of special nuclear material is desirable before the materials enters into the transportation infrastructure of the U.S. and interdiction becomes more complex. Radiation Portal Monitors (RPMs) are passive radiation detection systems implemented at over a thousand border crossings designed to determine if cargo contains any nuclear material in a safe, nondestructive and effective manner[?]. The Department of Homeland Security (DHS) continues to fund research through the Domestic Nuclear Detection Office (DNDO) in order to develop replacement technologies for the current ^3He RPMs as ^3He cannot be economically replaced. There are several alternatives to ^3He being considered, and all, with the exception of gas filled proportional detectors, involve the detection of neutrons from scintillation events of the energy deposited in the material from the neutron absorption reaction. These detectors (among other requirements outline in Table 1) must be able to effectively discriminate between gamma (which can occur in medical isotopes) and neutrons (indictive of special nuclear material).

Table 1: Replacement Detector Requirements [?]

Parameter	Specification
Absolute neutron detection efficiency	2.5 cps/ng of ^{252}Cf
Intrinsic gamma-neutron detection efficiency	$\epsilon_{int,\gamma n} \leq 10^{-6}$
Gamma absolute rejection ratio for neutrons (GARRn)	$0.9 \leq \text{GARRn} \leq 1.1$ at 10 mR/h exposure
Cost	\$ 30,000 per system

Neutron detectors often utilize a material doped with an isotope of large thermal cross section for absorption such as ^6Li or ^{10}B . When these materials absorb a neutron the nucleus of the isotope becomes unstable and fissions into reaction products. These reaction products (having an initial kinetic energy from the Q-value of the neutron absorption reaction) travel through the material, transferring their kinetic energy to the material. Photon interactions in the detector occur when a photon scatters off a single electron in a Compton scattering event (Table 2). This Compton electron then produces a cascade of secondary electrons in the material, which, depending upon the energy, may or may not deposit a majority of its energy in the detector. The difference in the transfer of kinetic energy from charged particle to electrons and from photon interactions (Compton scattering) to electrons introduces an opportunity to exploit the difference in energy deposition in order to maximize the discrimination between neutron and photon interactions in a detector.

Table 2: Maximum Energy of Secondary Electrons from Compton Scattering

	Photon Energy (MeV)	Maximum Compton Energy (MeV)
^{137}Cs	0.662	0.478
^{60}Co	1.17, 1.33	0.960, 1160

This document is organized as follows. A brief overview of the interaction of charged particles in matter will be provided in Section 2, as well as some preliminary experiments demonstrating the range of secondary electrons in neutron-gamma discrimination. The GEANT4 toolkit was used for the modeling of the energy deposition. Section 3 will provide an overview of the GEANT4 toolkit. Section 4 will provide details on how the GEANT4 toolkit was implemented for this particular simulation, as well as providing validation of the calculations performed by the GEANT4 toolkit in Section 5. In Section 6 the results of this model applied to a single film will demonstrate the enhanced ability of neutron-gamma discrimination through secondary electrons.

2 Previous Work

Previous work on the energy deposition of thin films focused on spectra measurements from fabricated films along with single collision energy loss spectra for physical insights. A sequence of 10% ^6LiF , 5% PPO-POPOP films in a PS matrix cast to thickness between 15 and 600 μm were fabricated and the response was measured from a gamma source as well as a neutron source. These experiment results are shown in 2.1. The single collision energy loss spectra was investigated for electrons in water in order to provide insight on the amount of energy an electron loses in a collision. These results are discussed in Section 2.2.

2.1 Spectra Measurements

Evidence that the secondary electrons contribute to energy loss can be seen in Figure 1 where there is an increase in the endpoint of the spectra as films become thicker. This increase in the spectra endpoint is indicative of the film producing more light, and as the light collection geometry remained constant, the increase in the endpoint is attributed to a larger energy deposition in the 50 μm film compared to the 15 μm or 25 μm film. Figure 2 shows the intrinsic efficiency of these film from spectra obtained from a ^{60}Co

(a) Beta (^{36}Cl) Spectra Endpoints for PS films (b) Gamma (^{60}Co) Spectra Averages for PS films

Figure 1: Spectra properties as a function of film thickness

source. As the film thickness increases the pulse height discriminator at which an intrinsic efficiency of one in a million ($\epsilon_{int,\gamma} \leq 10^{-6}$) is reached also increases. The neutron spectra (shown in the solid lines) does not increase in light yield with increasing thickness, further providing an indication that the thickness of the films can be optimized to maximize the neutron count rates¹ while minimizing the response of the detector to photons.

Figure 2: Gamma intrinsic efficiency (dashed lines) plotted against neutron counts (solid)

2.2 Single Collision Energy Loss

Single collision energy loss spectra provides the probability that that a given collision will result in an energy loss. Provided a spectra of secondary electrons from either the Compton scattered electron or the ^6Li reaction products it is then possible to determine the average energy loss per collision. A single collision energy loss spectra for water is shown in Figure 3. For low electron energies (< 50 eV) it is very probable that the electron will lose a majority of its energy in a single collision. More energetic electrons, however, tend to lose a lower fraction of there total energy. A Compton scattered photon, with an energy in the 100's of keV range, will then lose far less energy per collision than an electron in the low keV range liberated from the passage of a neutron reaction product through the material. When the average and median energy transfer are plotted

Figure 3: Single-collision energy loss spectra for electrons in water [?]

as a function of incident electron energy (Figure 4) the difference in the energy loss spectra becomes more apparent. For low energies (up to an incident electron energy of 100 eV) the average and median energy transfer are roughly equal to each other, about half of the incident electron. Past 100 eV average energy increases faster than the median energy transfer implying that while a few collisions result in large energy transfers most of the collisions do not. It is also interesting to note that the average and median do not increase linearly with the incident energy past 100 eV (the ordinate axis is a log scale). In fact, the average

¹The neutron count rate is increased with thickness by the increased mass of the detector

¹³¹ energy transferred per collision is mostly bounded by 60 eV even for incident electron energies of ~ 10 keV. This
¹³² is significant because it implies that high energy electrons from photon events will deposit a small fraction of
their energy in the material.

Figure 4: Average and median energy transfer in liquid water as functions of incident-electron energy [?]

133

3 Introduction to GEANT4

GEANT4 (GEometry ANd Tracking) is a free, open source, Monte Carlo based physics simulation toolkit developed and maintained at CERN widely used in the physics community [?, ?, ?]. It is based off of the existing FORTRAN based GEANT3, but updated to an object-oriented C++ environment based on an initiative started in 1993. The initiative grew to become an international collaboration of researchers participating in a range of high-energy physics experiments in Europe, Japan, Canada and the United States. As GEANT4 is a toolkit primarily developed for high energy physics, particles are designated according to the PDG (Particle Data Group) encoding. In addition, the physics processes are referenced according to the standard model. In the standard model particles are divided into two families, bosons (the force carriers such as photons) and fermions (matter). The fermions consist of both hadrons and leptons. Hadrons are particles composed of quarks which are divided into two classes: baryons (three quarks) and mesons (two quarks). Typical baryons include the neutron and the proton, while an example of a meson is the pion. An example of a lepton is the electron.

3.1 Organization of the GEANT4 Toolkit

The GEANT4 toolkit is divided into eight class categories:

- Run and Event - generation of events and secondary particles.
- Tracking and Track - transport of a particle by analyzing the factors limiting the step size and by applying the relevant physics models.
- Geometry and Magnetic Field - the geometrical definition of a detector (including the computation of the distances to solids) as well as the management of magnetic fields.
- Particle Definition and Matter - definition of particles and matter.
- Hits and Digitization - the creation of hits and their use for digitization in order to model a detector's readout response.
- Visualization - the visualization of a simulation including the solid geometry, trajectories and hits.
- Interface - the interactions between the toolkit and graphical user interfaces and well as external software.

There are then three classes which must be implemented by the user in order to use the toolkit. These classes are:

- `G4VUserDetectorConstruction` which defines the geometry of the simulation,
- `G4VUserPhysicsList` which defines the physics of the simulation, and
- `G4VUserPrimaryGeneratorAction` which defines the generation of primary events.

Five additional classes are available for further control over the simulation:

- `G4UserRunAction` which allows for user actions

3.2 GEANT4 Tracking and Secondaries

A GEANT4 simulation starts with a run which contains a set number of events. An event is a particular process of interest to the user, such as shooting a single particle at a detector. Typical usage might be to have a run firing 1,000 neutrons at a detector, where each neutron is a single event. Each particle transported in GEANT4 is assigned a unique track ID and a parent ID. The particle that initiates the event is given a parent ID of 0 and a track ID of 1. If the parent particle has a collision, and produces a secondary particle, this secondary particle is then given a parent ID of 1 (corresponding to the first secondary) and a track ID of

Expand this section

2. Secondaries are tracked in GEANT4 utilizing a stack in which the most recent secondary (and its cascade) is tracked first.

Listing 1 provides an example from the verbose output of GEANT4 of the tracking. The initial particle in the event is the neutron because it has a parent ID of 0. The alpha and triton are the secondaries produced by this collision. The alpha is assigned a parent ID of 1 (corresponding to the first generation) with a track ID of 3. The triton is also assigned a parent ID of 1, but with a track ID of 2.

Listing 1: Tracking Example

```

180 *****
181 * G4Track Information: Particle = neutron, Track ID = 1, Parent ID = 0
182 *****
183
184
185 Step#    X(mm)    Y(mm)    Z(mm) KinE(MeV)  dE(MeV)  StepLeng  TrackLeng  NextVolume  ProcName
186 0         0         0        -6.59  2.5e-08    0         0         0         Absorber  initStep
187 1         0         0        -3.64    0         0         2.95      2.95      Absorber  NeutronInelastic
188 :----- List of 2ndaries - #SpawnInStep= 2( Rest= 0, Along= 0, Post= 2), #SpawnTotal= 2 -----
189 :         0         0        -3.64    2.73      triton
190 :         0         0        -3.64    2.05      alpha
191 :----- EndOf2ndaries Info -----
192
193 *****
194 * G4Track Information: Particle = alpha, Track ID = 3, Parent ID = 1
195 *****
196
197 Step#    X(mm)    Y(mm)    Z(mm) KinE(MeV)  dE(MeV)  StepLeng  TrackLeng  NextVolume  ProcName
198 0         0         0        -3.64    2.05    0         0         0         Absorber  initStep
199 1 -0.000201 0.000128   -3.64    2.01    0.0491  0.000266  0.000266  Absorber  ionIoni
200 2 -0.00049 0.000312   -3.64    1.93    0.0705  0.000381  0.000647  Absorber  ionIoni
201
202 *****
203 * G4Track Information: Particle = triton, Track ID = 2, Parent ID = 1
204 *****
205
206 Step#    X(mm)    Y(mm)    Z(mm) KinE(MeV)  dE(MeV)  StepLeng  TrackLeng  NextVolume  ProcName
207 0         0         0        -3.64    2.73    0         0         0         Absorber  initStep
208 1 0.000339 -0.000215   -3.64    2.71    0.0116  0.000447  0.000447  Absorber  hIoni
209

```

4 Methods

A discussion of the steps necessary to implement the simulation of energy deposition in GEANT4 follows. This involved writing the code for the simulation, as well as correctly interpreting the output. As such, this section is organized by first examining the process of setting up the simulation and then will go into the analysis of the results from the toolkit.

4.1 GEANT4 Implementation

A large focus of this work was on creating a working simulation of the GEANT4 toolkit. Preliminary attempts were made to install GEANT4 on a Windows based machine linking to Microsoft Visual Studio. While these attempts were successful, a larger scale computing environment was desired. GEANT4 was then installed on the University of Tennessee's nuclear engineering computing cluster, along with the necessary visualization drivers and data files. Brief documentation on compiling simple examples on the cluster are available at the necluster wiki ². For convenience a subversion repository was created to manage the developed code base, and all source code is available by anonymous checkout from <http://www.murphs-code-repository.googlecode.com/svn/trunk/layeredPolymerTracking>. Revision 360 was the code base used to generate the results shown. The following section provides implementation specific details of the code base used to simulate the energy deposition in thin films. It is organized according to the three base classes that a user must implement in GEANT4, namely `G4VUserDetectorConstruction`, `G4VUserPhysicsList`, and `G4VUserPrimaryGeneratorAction`.

4.1.1 Detector Geometry

A detector geometry in GEANT4 is made up of a number of volumes. The largest volume is the `world` volume which contains all other volumes in the detector geometry. Each volume (an instance of `G4VPhysicalVolume`) is created by assigning a position, a pointer to the mother volume and a pointer to its mother volume (or `NULL` if it is the `world` volume). A volume's shape is described by `G4VSolid`, which has a shape and the specific values for each dimension. A volume's full properties is described by a logical volume. A `G4LogicalVolume` includes a pointer to the geometrical properties of the volume (the solid) along with physical characteristics including:

- the material of the volume,
- sensitive detectors of the volume and,
- any magnetic fields.

Listing 2 provides the implementation of the world physical volume. The geometry was set up such that it is possible to define multiple layers of detectors, as shown in Figure 6.

Listing 2: World Physical Volume

```
// World
worldS = new G4Box("World",worldSizeXY, worldSizeXY, worldSizeZ*0.5);
worldLV = new G4LogicalVolume(worldS,defaultMaterial,"World");
worldPV = new G4PVPlacement(0,G4ThreeVector(),worldLV,"World",0,false,0,fCheckOverlaps);
```

The detector was described by creating creating a single layer of neutron absorber and gap material and placing it in another volume (the calorimeter). The containing volume (calorimeter) was placed inside of the the physical world (Listing 3).

Listing 3: Calorimeter Volume

```
// Calorimeter (gap material)
caloS = new G4Tubs("Calorimeter",iRadius,oRadius,caloThickness/2,startAngle,spanAngle);
```

²It should be noted that this example uses the CMAKE build system (as per the GEANT4 recommendation) but a large majority of the examples still use GNUmake for building. This can be accomplished by adding `source /opt/geant4/geant4-9.5p1/share/Geant4-9.5.1/geant4make/geant4make.sh` to the user's `.bashrc`.

```

253     caloLV = new G4LogicalVolume(caloS, gapMaterial, "Calorimeter");
254     caloPV = new G4PVPlacement(0, G4ThreeVector(), caloLV, "Calorimeter", worldLV, false, 0,
255                               fCheckOverlaps);
256

```

The `calorimeter` was the mother volume for each layer. The code was developed such that the simulation of multiple layers can be easily set at compile time or by utilizing a run macro through the `DetectorMessenger` class. Multiple repeated volume can be achieved in GEANT4 through `G4PVReplica` or `G4PVParameterised`. As each of the layers had the same geometry, `G4PVReplica` was chosen as the implementation (Listing 4).

Listing 4: Layer Volume

```

261 // Layer (Consists of Absorber and Gap)
262 layerS = new G4Tubs("Layer", iRadius, oRadius, layerThickness/2, startAngle, spanAngle);
263 layerLV = new G4LogicalVolume(layerS, defaultMaterial, "Layer");
264 if (nofLayers > 1){
265     layerPV = new G4PVReplica("Layer", layerLV, caloLV, kZAxis, nofLayers, layerThickness, -
266                               caloThickness/2);
267 }else{
268     layerPV = new G4PVPlacement(0, G4ThreeVector(0.0, 0.0, 0.0), layerLV, "Layer", caloLV,
269                               false, 0, fCheckOverlaps);
270 }
271

```

Finally, the neutron absorber and gap material were defined as single cylinders which were then placed in the layer mother volume (Listing 5). The size of these solids (and the materials) could be set either at compile time through `DetectorConstruction` constructor or by using the `DetectorMessenger` in the run macro. Figure 6 shows a rendering of the 10 layers of the detector with the trajectories from a gamma event.

Listing 5: Absorber and Gap Volumes

```

277 // Absorber
278 absS = new G4Tubs("Abso", iRadius, oRadius, absThickness/2, startAngle, spanAngle);
279 absLV = new G4LogicalVolume(absS, absMaterial, "Absorber", 0);
280 absPV = new G4PVPlacement(0, G4ThreeVector(0.0, 0.0, -gapThickness/2), absLV, "Absorber",
281                           layerLV, false, 0, fCheckOverlaps);
282
283 // Gap
284 gapS = new G4Tubs("Gap", iRadius, oRadius, gapThickness/2, startAngle, spanAngle);
285 gapLV = new G4LogicalVolume(gapS, gapMaterial, "Gap", 0);
286 gapPV = new G4PVPlacement(0, G4ThreeVector(0.0, 0.0, absThickness/2), gapLV, "Gap", layerLV,
287                           false, 0, fCheckOverlaps);
288

```

Figure 5: World, Calorimeter, Layer and Absorber and Gap

Figure 6: 10 Layer Detector with a simulated gamma event

4.1.2 Physics Lists

The user of the GEANT4 toolkit is responsible for selecting the proper physics processes to model in the `PhysicsList`. This is unlike other transport codes (such as MCNPX) where basic physics are enabled by default and the user only has select the appropriate cards. However, GEANT4 does provide examples of implemented `PhysicsLists` as well as modular physics lists which provide a way to construct a physics list by combing physics list. Thus, extensive use of `G4ModularPhysicsList` was employed to handle the assigning of the physics processes to each particle in the correct order. The physics lists chosen for this simulation are listed below:

- `G4EmStandardPhysics` The electromagnetic physics defines the electrons, muons, and taus along with their corresponding neutrinos. For electrons, the primary concern of this simulation, multiple scattering,

electron ionization, and electron bremsstrahlung processes were assigned. In addition the positron is defined and the multiple scattering process, electron ionization process, electron bremsstrahlung process and positron annihilation is assigned [?].

- **G4EmLivermorePhysics** The Livermore physics process extend the **EMStandardPhysics** down to low (250 eV) energies. Even lower energies can be reached by including **G4DNAPhysics**. The physics processes extended with **G4EmLivermorePhysics** are the photo-electric effect, Compton scattering, Rayleigh scattering, gamma conversion, Ionisation and Bremsstrahlung[?].
- **HadronPhysicsQGSP_BERT_HP** Hadronic physics are included to model the nuclear interactions. The chosen list is a Quark Gluon String Model for energies in the 5-25 GeV range, with a Bertini cascade model until 20 MeV. Once a hadron has an energy of 20 MeV the high precision cross section driven models are applied[?].
- **G4IonPhysics** Finally, to handle the transport of the charged ions resulting from an ${}^6\text{Li}(n, \alpha){}^3\text{H}$ interaction the **G4IonPhysics** list was used.

Listing 6: Implemented Physics List

```

313 /**
314  * PhysicsList
315  *
316  *
317  * Constructs the physics of the simulation
318  */
319 PhysicsList::PhysicsList() : G4VModularPhysicsList() {
320     currentDefaultCut = 10*nm;
321
322     // Adding Physics List
323     //RegisterPhysics( new G4EmDNAPhysics());
324     RegisterPhysics( new G4EmStandardPhysics());
325     RegisterPhysics( new G4EmLivermorePhysics());
326     RegisterPhysics( new HadronPhysicsQGSP_BERT_HP());
327     RegisterPhysics( new G4IonPhysics());
328 }

```

Finally, the default cut range was decreased from 1 cm to 1 nm in **SetCuts()** (Listing 7)

Listing 7: Implemented Physics List

```

331
332 void PhysicsList::SetCuts(){
333     SetDefaultCutValue(10*nm);
334 }

```

4.1.3 Primary Event Generator

The user is responsible for telling the simulation toolkit the primary event to generate. While there is great flexibility to generate any source distribution, a particle gun was chosen for simplicity. **G4ParticleGun** generates primary particle(s) with a given momentum and position without any randomization. The implementation of this is shown in Listing 8.

Listing 8: Primary Event Generator

```

341 PrimaryGeneratorAction::PrimaryGeneratorAction() : G4VUserPrimaryGeneratorAction(),
342     fParticleGun(0) {
343     G4int nofParticles = 1;
344     fParticleGun = new G4ParticleGun(nofParticles);
345
346     // default particle kinematic
347     G4ParticleDefinition* particleDefinition = G4ParticleTable::GetParticleTable()->
348         FindParticle("e-");
349     fParticleGun->SetParticlePosition(G4ThreeVector(0.,0.,0.0));
350     fParticleGun->SetParticleDefinition(particleDefinition);
351     fParticleGun->SetParticleMomentumDirection(G4ThreeVector(0.,0.,1.));
352 }

```

```

353 0   fParticleGun->SetParticleEnergy(50.*MeV);
354   }
355

```

Actual primary particles are generated with `GeneratePrimaries`, which uses the `G4ParticleGun` to determine the vertex of the primary event.

Listing 9: Generate Primaries

```

358 void PrimaryGeneratorAction::GeneratePrimaries(G4Event* anEvent)
359 {
360 2 // This function is called at the beginning of event
361
362 4 // In order to avoid dependence of PrimaryGeneratorAction
363 // on DetectorConstruction class we get world volume
364 6 // from G4LogicalVolumeStore
365 G4double worldZHalfLength = 0;
366 8 G4LogicalVolume* worlLV = G4LogicalVolumeStore::GetInstance()->GetVolume("World");
367 G4Box* worldBox = 0;
368 0 if ( worlLV) worldBox = dynamic_cast< G4Box*>(worlLV->GetSolid());
369 if ( worldBox ) {
370 2     worldZHalfLength = worldBox->GetZHalfLength();
371 }
372 4 else {
373     G4cerr << "World volume of box not found." << G4endl;
374 6     G4cerr << "Perhaps you have changed geometry." << G4endl;
375     G4cerr << "The gun will be place in the center." << G4endl;
376 8 }
377
378 0 // Set gun position
379 fParticleGun->SetParticlePosition(G4ThreeVector(0., 0., -worldZHalfLength+1*cm));
380 2 fParticleGun->GeneratePrimaryVertex(anEvent);
381 }
382 4
383

```

4.2 Sensitive Detectors and Hits

GEANT4 offers a myriad of different ways to output the results of a simulation. It is possible to write out every track with the `Verbose = 1` option, create `MultiFunctionalDetector` and `G4VPrimitiveScorer`, or implement a hit and readout based approach [?]. Previous GEANT4 experience included `G4VHit` and `G4VSensitiveDetector`, so this approach was used in this simulation. A hit is defined to be a snapshot of the physical interaction of a track in a sensitive region of a detector. As the user is responsible for implementing `G4VHit` the hit can contain any information about the step, including:

- the position and time of the step,
- the momentum and energy of the track,
- the energy deposition of the step,
- or information about the geometry.

For this simulation any information about the particle that could be recorded was recorded. This included the energy deposition, position of the hit, momentum, kinetic energy, track ID, parent ID, particle definition, volume and copy number (Listing 10).

Listing 10: Calorimeter Hit

```

398 /**
399  * @brief - Hit: a snapshot of the physcial interaction of a track in the sensitive region
400 2   of a detector
401  *
402  * Contians:
403 4  * - Particle Information (type and rank (primary, secondary, tertiary ...))
404  * - Positon and time
405 6  * - momentum and kinetic energy
406

```

```

407 8  * - deposition in volume
408 8  * - geometric information
409 0  */
410 8  class CaloHit : public G4VHit {
411 2  public:
412 8      CaloHit(const G4int layer);
413 4      ~CaloHit();
414
415 6      inline void* operator new(size_t);
416 8      inline void operator delete(void*);
417 8      void Print();
418
419 0  private:
420 8      G4double edep;                /* Energy Deposited at the Hit */
421 2      G4ThreeVector pos;           /* Position of the hit */
422 8      G4double stepLength;         /* Step Length */
423 4      G4ThreeVector momentum;     /* Momentum of the step */
424 8      G4double kEnergy;            /* Kinetic Energy of the particle */
425 6      G4int trackID;              /* Track ID */
426 8      G4int parentID;             /* Parent ID */
427 8      G4ParticleDefinition* particle; /* Particle Definition */
428 8      G4int particleRank;          /* Primary, Secondary, etc */
429 0      G4VPhysicalVolume* volume;   /* Physical Volume */
430 8      G4int layerNumber;          /* Copy Number of Layer */
431 2
432 8  public:
433 4      // Setter and Getters
434 8  };
435 6
436 8  typedef G4THitsCollection<CaloHit> CaloHitsCollection;
437 8  extern G4Allocator<CaloHit> HitAllocator;
438
439 0  inline void* CaloHit::operator new(size_t){
440 8      void *aHit;
441 2      aHit = (void *) HitAllocator.MallocSingle();
442 8      return aHit;
443 4  }
444
445 6  inline void CaloHit::operator delete(void *aHit){
446 8      HitAllocator.FreeSingle((CaloHit*) aHit);
447 8  }
448

```

449 The G4VSensitiveDetector is attached to a logical volume and is responsible for filling the hit collection.
450 This is accomplished in ProcessHits of CaloSensitiveDetector (Listing 11).

Listing 11: Sensitive Detector

```

451 /**
452 8  * ProcessHits
453 2  *
454 8  * Adds a hit to the sensitive detector, depending on the step
455 4  */
456 8
457 6  G4bool CaloSensitiveDetector::ProcessHits(G4Step* aStep, G4TouchableHistory*){
458 8
459 8      G4double edep = aStep->GetTotalEnergyDeposit();
460 8      G4double stepLength = aStep->GetStepLength();
461 0
462 8      // Getting the copy number
463 2      G4TouchableHistory* touchable = (G4TouchableHistory*)
464 8          (aStep->GetPreStepPoint()->GetTouchable());
465 4      G4int layerIndex = touchable->GetReplicaNumber(1);
466 8
467 6      // Creating the hit
468 8      CaloHit* newHit = new CaloHit(layerIndex);
469 8      newHit->SetTrackID(aStep->GetTrack()->GetTrackID());
470 8      newHit->SetParentID(aStep->GetTrack()->GetParentID());
471 0      newHit->SetEdep(edep);
472 8      newHit->SetStepLength(stepLength);

```



```

473:2    newHit->SetPosition(aStep->GetPreStepPoint()->GetPosition());
474    newHit->SetLayerNumber(layerIndex);
475:4    newHit->SetMomentum(aStep->GetPreStepPoint()->GetMomentum());
476    newHit->SetKineticEnergy (aStep->GetPreStepPoint()->GetKineticEnergy());
477:6    newHit->SetParticle(aStep->GetTrack()->GetDefinition());
478    newHit->SetVolume(aStep->GetTrack()->GetVolume());
479:8
480    // Adding the hit to the collection
481:0    hitCollection->insert( newHit );
482
483:2    return true;
484
485 }

```

486 The simulation was designed so that a separate sensitive detector was assigned to the gap and absorber.
 487 While this is not strictly necessary as the geometric position determines what layer of the gap or absorber
 488 the hit occurred in, this made the analysis code easier to write. A separate method was written in
 489 `DetectorConstruction` to create the sensitive detectors and assign them to the proper logical volumes
 490 (Listing 12) `SetSensitiveDetectors()` is called from the the constructor of `DetectorConstruction`.

Listing 12: Creating Sensitive Detectors

```

491
492:1 /**
493    * SetSensitiveDetectors
494:3    *
495    * Setting the Sensitive Detectors of the Detector
496:5    */
497 void DetectorConstruction::SetSensitiveDetectors(){
498:7     G4SDManager* SDman = G4SDManager::GetSDMpointer();
499     absSD = new CaloSensitiveDetector("SD/AbsSD", "AbsHitCollection");
500:9     SDman->AddNewDetector(absSD);
501     absLV->SetSensitiveDetector(absSD);
502:1
503     gapSD = new CaloSensitiveDetector("SD/GapSD", "GapHitCollection");
504:3     SDman->AddNewDetector(gapSD);
505     gapLV->SetSensitiveDetector(gapSD);
506
507 }

```

508 4.3 Analysis

509 Analysis of hit collection was preformed with ROOT. Once again there are other options (notably Open-
 510 Scientist) but previous experience was why ROOT was selected as the base for the Analysis framework. A
 511 singleton class was written for the analysis which processed the hit collections, assigning the various results
 512 to root histograms. User action classes `EventAction` and `RunAction` are called at the beginning and end of
 513 each run and event, respectively (Listing 13,14). These classes allowed for the analysis code to be independent
 514 of the simulation.

Listing 13: Event Action

```

515
516:1 EventAction::EventAction() : G4UserEventAction(){
517    // Nothing to be Done Here
518:3 }
519
520:5 /**
521    * BeginOfEventAction
522:7    *
523    * @param const G4Event* event - event to be processed
524:9    *
525    * At the begining of an event we want to clear all the event
526:1    * accumulation variables.
527    */
528:3 void EventAction::BeginOfEventAction(const G4Event* event){
529    Analysis::GetInstance()->PrepareNewEvent(event);
530:5 }
531

```

```

532 7 /**
533  * EndOfEventAction
534 9 *
535  * @param const G4Event* event - event to be processed
536 1 *
537  * At the end of an event we want to call analysis to process
538 3 * this event, and record the useful information.
539  */
540 5 void EventAction::EndOfEventAction(const G4Event* event){
541  Analysis::GetInstance()->EndOfEvent(event);
542 7 }

```

Listing 14: Run Action

```

544 RunAction::RunAction() : G4UserRunAction(){ }
545 1
546
547 3 void RunAction::BeginOfRunAction(const G4Run* run){
548  G4cout<<"Starting run: " << run->GetRunID()<< G4endl;
549 5 Analysis::GetInstance()->PrepareNewRun(run);
550  }
551 7
552 void RunAction::EndOfRunAction(const G4Run* aRun){
553 9 Analysis::GetInstance()->EndOfRun(aRun);
554  }
555

```

4.4 Determination of Energy Deposition

The energy deposition of an event is calculated by the sum of all of the energy deposited by individual hits in the sensitive detector (Equation 1). While it is possible to break down the energy deposition by which physics process caused the deposition, this was not implemented in order to avoid over complication.

$$E_{\text{dep,event}} = \sum E_{\text{dep,hit}} \quad (1)$$

`ProcessHitCollection` is called at the end of each event (Listing 15). Each hit is accessed and the layer at which it occurs is determined³. In addition the name of the volume is determined, and the energy deposition of the hit is added to the energy deposition of the event. If the hit occurred in the `absorber` layer and the particle is an electron the kinetic energy of that hit is also recorded.

Listing 15: Process Hit Collection

```

561 /**
562 1 * ProcessHitCollection
563  *
564 3 *
565  * @param G4VHitsCollection *hc
566 5 */
567 void Analysis::ProcessHitCollection(G4VHitsCollection *hc,G4int eventID){
568 7
569  // Looping through the hit collection
570 9 G4double hitColEdepTot_Abs[NUMLAYERS+1]; // Total EDep (abs) for Hit Collection
571  G4double hitColEdepTot_Gap[NUMLAYERS+1]; // Total EDep (gap) for Hit Collection
572 1 G4int PID; // Parent ID
573  for(int i= 0; i < NUMLAYERS+1; i++){
574 3 hitColEdepTot_Abs[i] = 0.0;
575  hitColEdepTot_Gap[i] = 0.0;
576 5 }
577
578 7 // Energy Deposition of the event
579  for(G4int i = 0; i < hc->GetSize(); i++){
580 9 CaloHit* hit = (CaloHit*) hc->GetHit(i);
581
582 1 G4double eDep = hit->GetEdep();

```

³C arrays start at 0, so memory is allocated for one more than the total number of layers. This allows for `NUMLAYERS+1` to be used an index into the histogram for the total of all layers in the material (either `gap` or `absorber`).

```

583         G4int layerNum = hit->GetLayerNumber();
584:3         if (strcmp(hit->GetVolume()->GetName(), "Gap")){
585             // Hit occurred in the Gap
586:5             hitColEDepTot_Gap[layerNum] += eDep;
587             (hHitTotEDepGap[layerNum])->Fill(eDep);
588:7         }else if(strcmp(hit->GetVolume()->GetName(), "Absorber")){
589             // Hit occurred in the Abs
590:9             hitColEDepTot_Abs[layerNum] += eDep;
591             (hHitTotEDepAbs[layerNum])->Fill(eDep);
592:1
593             /* Is this a secondary electron of the event? */
594:3             if(hit->GetParticle()->GetPDGEncoding() == 11){
595                 PID = hit->GetParentID();
596:5                 if (PID < NUMPID){
597                     (hSecElecKinAbs[layerNum][PID])->Fill(hit->GetKineticEnergy());
598:7                 }
599             }
600:9         }
601         else{
602:1             G4cout<<"ERROR - Unkown Volume for sensitive detector"<<G4endl;
603         }
604:3     }
605
606:5     // Adding this Hit collection's energy deposited to event total
607     for (int i = 0; i < NUMLAYERS; i++){
608:7         // Incrementing each individual bin
609         eventEDepTot_Abs[i] += hitColEDepTot_Abs[i];
610:9         eventEDepTot_Gap[i] += hitColEDepTot_Gap[i];
611
612:1         // Last bin is Calorimeter Total (all Abs layers and all Gap layers)
613         eventEDepTot_Abs[NUMLAYERS] += hitColEDepTot_Abs[i];
614:3         eventEDepTot_Gap[NUMLAYERS] += hitColEDepTot_Gap[i];
615     }
616:5 }

```

618 Finally, a run macro was written to control the entire run (Listing 16). The material and thickness
619 of the detector are declared (made possible by the use of `DetectorMessenger`), and then the detector is
620 dynamically updated. A ^{60}Co source is simulated by shooting photons of the 1.1732 MeV and 1.3325 MeV.
621 The source particle is then changed to a neutron, and thermal (0.025 eV) neutrons are shot at the detector.
622 The thickness of the absorber is then increased, the geometry updated, and the entire process repeated. As
623 these runs tend to take a large amount of time, GEANT4 was parallelized for use with MPI to take advantage
624 of the cluster computing power.

Listing 16: Run Macro

```

625 #
626:1 /tracking/verbose 0
627 #
628:3 # Setting up the detector
629 #
630:5 #
631 /PolymerTransport/det/setAbsMat PS_Detector
632:7 /PolymerTransport/det/setGapMat G4_POLYSTYRENE
633 /PolymerTransport/det/setGapThick 0.3175 cm
634:9 #
635 /PolymerTransport/det/setAbsThick 15 um
636:1 /PolymerTransport/det/update
637 # Cobalt 60
638:3 /gun/particle gamma
639 /gun/direction 0 0 1
640:5 /gun/energy 1.1732 MeV
641 /run/beamOn 500000000 # 500 Million
642:7 /gun/energy 1.3325 MeV
643 /run/beamOn 500000000 # 500 Million
644:9 # Neutron
645 /gun/particle neutron
646:1 /gun/energy 0.025 eV
647 /run/beamOn 1000000 # 1 Million

```

```
648: #  
649 /PolymerTransport/det/setAbsThick 25 um  
650 /PolymerTransport/det/update  
651
```

5 Simulation Validation

GEANT4 is a toolkit implemented by the user so extensive efforts were completed in order to validate the results and ensure no bugs exists. First steps were taken (for small runs) to compute the energy deposition for small runs by hand in order to make sure they agreed with the analysis code. In addition the reaction products of the ${}^6\text{Li}(n, \alpha){}^3\text{H}$ were checked to make sure that they agreed with the published values⁴. The GEANT4 simulation was validated by comparing the single collision energy loss spectra in water and by comparing the simulation energy deposition to that of a measured spectra.

5.1 Energy Deposition Validation

The energy deposition was tested by reproducing the single collision energy loss spectra in water⁵. The `PhysicsList` was extended to include `G4DNAPhysics` and the detector material was set to the NIST definition contained in the toolkit with `G4Material* H2O = man->FindOrBuildMaterial("G4_WATER")`. In general there was excellent agreement between the simulated energy spectra and a previously published spectra[?]. The simulated spectra had much better resolution at fine energies (corresponding to discrete states) of which Turners did not.

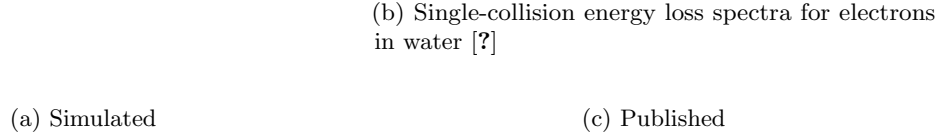


Figure 7: Single Collision Energy Loss of Water

5.2 Spectra Validation

The simulated energy deposition is not the directly equivalent to light collected on the PMT because the scintillation process and light collection is not modeled. However, it is well known that scintillation follows the energy deposition[?]. Thus, up to scaling constants, the energy deposition can be considered equivalent to the scintillation and representative of the measured spectra. Rather than attempting to back out these scaling constants the weighted average of spectra were used in which integration and normalization removes these fudge factors. The simulation was validated by computing the weighted average of the energy deposition² and comparing it to the spectra average defined in 3. There is excellent agreement between the measured gamma weighted average (right ordinate axis) and the average energy deposition from a ${}^{60}\text{Co}$ source (left ordinate axis). Non-linearity is observed for films less than 200 μm , this is evidence that the cascade electrons from the Compton electron are energetic enough that the range of the electrons is much greater than the thickness of the film and leave the film without colliding to an energy in which the energy deposition is linear (Figure 4).

$$\langle E \rangle = \frac{\int_0^\infty \phi(E) E dE}{\int_0^\infty \phi(E) dE} \text{ where} \quad (2)$$

$$\langle \mu \rangle = \frac{\int_0^\infty f(x) x dx}{\int_0^\infty f(x) dx} \text{ where} \quad (3)$$

The comparison between the average energy deposition and measured channel allows for the a relationship to be drawn between the energy deposited and the channel number. This is completed by an taking an average

⁴GEANT4 4.9.2.p01 contains an error in which extra photons are generated, This has been fixed in the release used, 4.9.5p1

⁵An analysis class was not written for this simulation. Instead the verbosity of the simulation was set to `verbose=1` in the run macro. The first ionisation collision (`e-G4DNAIonisation`) was then extracted with `sed -n '/ParentID = 0/,/e-G4DNAIonisation/p' G4OutputFileName.txt | grep "e-_G4DNAIonisation" | awk '{print $5}'`

Figure 8: Gamma Simulation Agreement

Figure 9: Neutron Simulation Agreement

of the ratio between the average channel number (Equation 3 and the average energy deposition (Equation 2). This ratio is defined in Equation 4. This quantity is defined seperately for neturons and gammas.

$$\eta = \sum_t \frac{\langle E \rangle}{\langle \mu \rangle} \quad (4)$$

6 Results

6.1 Energy Deposition

The energy deposition was calculated for neutron and gamma events for films of thickness of 15 μm , 25 μm , 50 μm , 150 μm , 300 μm , 600 μm , 1 mm and 1 cm (Figure 10, 11).

Photons have a very low probability of interacting in the film due to polymer film being a low z -material. This is reflected in the majority of the events not interacting at all; about 1 in 10,000 of the events deposit energy in the film as seen in Figure 10. Several classic features of the spectra are apparent on the 1 cm thick film. These included the photo-peak in which all of the incident energy of the ^{60}Co is deposited in the film, as well as the individual Compton edges of the two photons from ^{60}Co . These features are not visible on the measured spectra due to the poor energy resolution of these films. There is also physical evidence of a lack of a Compton edge on the thinner films, but the films greater than 150 μm thick show some feature around 0.2 MeV. Films thinner than 150 μm show a very small amount of energy deposition that quickly tails off for higher energies, indicating that when a photon interaction occurs in the film the electrons from that interaction leave the film and the only energy deposition occurs from small ionizations as the highly energetic electron leaves the film material. It is also observed that the thinnest film (15 μm) has an average energy deposition of around 10 keV, while the 1 cm film has an average energy deposition of around 150 keV. The simulated energy deposition for neutron interactions in thin films is shown in Figure

Figure 10: Simulated Energy Deposition for a Single Film (gammas)

11. Several features of the spectra can be immediately noted. For thick films (1 cm) there is a very high probability that a given event will deposit all of its energy in the film (as expected). Thinner films have a smaller probability of depositing all of their energy, but this is overshadowed by the thick samples when plotted. It is also interesting to note that it is possible to observe the comparative effects of the α and ^3H in the neutron energy deposition spectra. The triton has a much shorter range ($\sim 10 \mu\text{m}$ in PS [?]) than the α (60 μm) so it has a higher probability of depositing all of its energy. Thus, for energies above 2.73 MeV (the energy of the triton) there is a higher probability of energy deposition (by about a factor of 10). These events are still very infrequent compared to the probability of depositing all of the reaction product energy. Even for the 15 μm the average energy deposition was above 50% of the total Q -value of the reaction, and by 200 μm this average energy deposited approaches 95% of the total 4.78 MeV.

Figure 11: Simulated Energy Deposition for a Single Film (neutrons)

6.2 Secondary Electron Energy Distribution

The distribution of secondary electrons from photon interactions are plotted in Figure 12. From these results it can be concluded that it is unlikely (around 1 in 10,000) that an electron will be scattered with the maximum Compton scattering kinetic energy, but rather have an energy somewhat lower than that. The distribution of secondary electrons from photon interactions is actually very flat, implying that it is likely for the electron from a Compton scattering event to have an energy in the 100's of keV. The distribution of the next generation of electrons was also calculated, and this distribution was also quite energetic (with a maximum energy corresponding to 0.55 MeV) but with a much large probability of having a collision that produces an electron with a much lower energy.

(a) First Secondary Electron

(b) Second Secondary Electron

Figure 12: Simulated kinetic energies of electrons from ^{60}Co interactions

7 Conclusions

GEANT4 has been employed to simulate the energy spectra of electrons and energy deposition from thermal neutrons and ^{60}Co gammas. A versatile implementation of the geometry was used in which it is possible to dynamically set the materials, thickness, and number of layers between runs. In addition, analysis methods have been written to aid in the reporting of the results. This simulation was verified by reproducing the single collision energy loss spectra for water, and also by comparing the average energy deposited to the measured average channel number for film ranging from $15\mu\text{m}$ to $600\mu\text{m}$.

The energy deposition of the films were calculated and plotted in Figure 11 and Figure 10. It is then observable that the gamma interactions have a very low probability of depositing a majority of the energy from a ^{60}Co photon into the material, while neutrons tend to deposit over 50% of their energy in the material for a $15\mu\text{m}$ film, and increasing to 96% for a 1 cm thick film. Figure 13 shows the average energy deposition as a function of thickness for neutrons and gammas, along with the calculated channel number (according to Equation 4). At thickness of less than $200\mu\text{m}$ there is significant separation between the average energy deposited by neutron events compared to gamma events. As the thickness of the films increased the average neutron energy approached the asymptotic limit of 4.78 MeV, while the average gamma energy increased. This creates less separation between the two, and provides less of an ability for neutron-gamma discrimination based on pulse height.

(a) Energy Deposition

(b) Estimated Channel Number

Figure 13: Comparison between average neutron and gamma energy deposition

References

- [1] CPB, “On a typical day in fiscal year 2011 CBP.” <http://www.cbp.gov/xp/cgov/about/>, 2012.
- [2] R. T. Kouzes, J. H. Ely, L. E. Erikson, W. J. Kernan, A. T. Lintereur, E. R. Siciliano, D. L. Stephens, D. C. Stromswold, R. M. Van Ginhoven, and M. L. Woodring, “Neutron detection alternatives to ^3He for national security applications,” *Nuclear Instruments and Methods in Physics Research Section A: Accelerators, Spectrometers, Detectors and Associated Equipment*, vol. 623, pp. 1035–1045, Nov. 2010.
- [3] R. Kouzes, J. Ely, A. Lintereur, and D. Stephens, “Neutron detector gamma insensitivity criteria,” *PNNL 18903*, 1999.
- [4] J. E. Turner, H. G. Paretzke, R. N. Hamm, H. A. Wright, and R. H. Ritchie, “Comparative study of electron energy deposition and yields in water in the liquid and vapor phases,” *Radiation Research*, vol. 92, pp. 47–60, Oct. 1982. ArticleType: research-article / Full publication date: Oct., 1982 / Copyright 1982 Radiation Research Society.
- [5] S. Agostinelli, J. Allison, K. Amako, J. Apostolakis, H. Araujo, P. Arce, M. Asai, D. Axen, S. Banerjee, G. Barrand, F. Behner, L. Bellagamba, J. Boudreau, L. Broglia, A. Brunengo, H. Burkhardt, S. Chauvie, J. Chuma, R. Chytrcek, G. Cooperman, G. Cosmo, P. Degtyarenko, A. Dell’Acqua, G. Depaola, D. Dietrich, R. Enami, A. Feliciello, C. Ferguson, H. Fesefeldt, G. Folger, F. Foppiano, A. Forti, S. Garelli, S. Giani, R. Giannitrapani, D. Gibin, J. Gomez Cadenas, I. Gonzalez, G. Gracia Abril, G. Greeniaus, W. Greiner, V. Grichine, A. Grossheim, S. Guatelli, P. Gumplinger, R. Hamatsu, K. Hashimoto, H. Hasui, A. Heikkinen, A. Howard, V. Ivanchenko, A. Johnson, F. Jones, J. Kallenbach, N. Kanaya, M. Kawabata, Y. Kawabata, M. Kawaguti, S. Kelner, P. Kent, A. Kimura, T. Kodama, R. Kokoulin, M. Kossov, H. Kurashige, E. Lamanna, T. Lampn, V. Lara, V. Lefebvre, F. Lei, M. Liendl, W. Lockman, F. Longo, S. Magni, M. Maire, E. Medernach, K. Minamimoto, P. Mora de Freitas, Y. Morita, K. Murakami, M. Nagamatsu, R. Nartallo, P. Nieminen, T. Nishimura, K. Ohtsubo, M. Okamura, S. O’Neale, Y. Oohata, K. Paech, J. Perl, A. Pfeiffer, M. Pia, F. Ranjard, A. Rybin, S. Sadilov, E. Di Salvo, G. Santin, T. Sasaki, N. Savvas, Y. Sawada, S. Scherer, S. Sei, V. Sirotenko, D. Smith, N. Starkov, H. Stoecker, J. Sulkimo, M. Takahata, S. Tanaka, E. Tcherniaev, E. Safai Tehrani, M. Tropeano, P. Truscott, H. Uno, L. Urban, P. Urban, M. Verderi, A. Walkden, W. Wander, H. Weber, J. Wellisch, T. Wenaus, D. Williams, D. Wright, T. Yamada, H. Yoshida, and D. Zschiesche, “Geant4a simulation toolkit,” *Nuclear Instruments and Methods in Physics Research Section A: Accelerators, Spectrometers, Detectors and Associated Equipment*, vol. 506, pp. 250–303, July 2003.
- [6] G. Collaboration, “Geant4 user’s guide for application developers.” <http://geant4.web.cern.ch/geant4/UserDocumentation/UsersGuides/ForApplicationDeveloper/html/index.html>, Dec. 2011. Version geant4 9.5.0.
- [7] J. Allison, K. Amako, J. Apostolakis, H. Araujo, P. Dubois, M. Asai, G. Barrand, R. Capra, S. Chauvie, R. Chytrcek, G. Cirrone, G. Cooperman, G. Cosmo, G. Cuttone, G. Daquino, M. Donszelmann, M. Dressel, G. Folger, F. Foppiano, J. Generowicz, V. Grichine, S. Guatelli, P. Gumplinger, A. Heikkinen, I. Hrivnacova, A. Howard, S. Incerti, V. Ivanchenko, T. Johnson, F. Jones, T. Koi, R. Kokoulin, M. Kossov, H. Kurashige, V. Lara, S. Larsson, F. Lei, O. Link, F. Longo, M. Maire, A. Mantero, B. Mascialino, I. McLaren, P. Lorenzo, K. Minamimoto, K. Murakami, P. Nieminen, L. Pandola, S. Parlati, L. Peralta, J. Perl, A. Pfeiffer, M. Pia, A. Ribon, P. Rodrigues, G. Russo, S. Sadilov, G. Santin, T. Sasaki, D. Smith, N. Starkov, S. Tanaka, E. Tcherniaev, B. Tome, A. Trindade, P. Truscott, L. Urban, M. Verderi, A. Walkden, J. Wellisch, D. Williams, D. Wright, and H. Yoshida, “Geant4 developments and applications,” *Nuclear Science, IEEE Transactions on*, vol. 53, pp. 270–278, Feb. 2006.
- [8] CERN, “Physics lists EM constructors in geant4 9.3.” <http://geant4.cern.ch/geant4/collaboration/working-groups/electromagnetic/physlist9.3.shtml>, Feb. 2012.
- [9] CERN, “Reference physics lists.” http://geant4.cern.ch/support/proc_mod_catalog/physics_lists/referencePL.shtml, Oct. 2008.

768
769

[10] CERN, “Detector definition and response.” <http://geant4.web.cern.ch/geant4/UserDocumentation/UsersGuides/ForApplicationDeveloper/html/ch02.html>, 2012.

770
771

[11] J. B. Birks, “Scintillations from organic crystals: Specific fluorescence and relative response to different radiations,” *Proceedings of the Physical Society. Section A*, vol. 64, pp. 874–877, Oct. 1951.

772
773
774

[12] H. Kudo and K. Tanaka, “Recoil ranges of 2.73 MeV tritons and yields of ^{18}F produced by the $^{16}\text{O}(\text{t},\text{n})^{18}\text{F}$ reaction in neutron-irradiated lithium compounds containing oxygen,” *The Journal of Chemical Physics*, vol. 72, no. 5, p. 3049, 1980.